Temperature dependent two-body abrasive wear of polycarbonate surfaces

Temperature dependent two-body abrasive wear of polycarbonate surfaces

Tarek Kershah[1,2], Stan F.S.P. Looijmans[1,2], Patrick D. Anderson[1], Lambèrt C.A. van Breemen[1*]

[1] *Polymer Technology, Department of Mechanical Engineering, Materials Technology Institute, Eindhoven University of Technology, P.O. Box 513, 5600 MB Eindhoven, The Netherlands*

[2] *Dutch Polymer Institute (DPI), P.O. Box 902, 5600 AX Eindhoven, The Netherlands*

Abstract

During the lifetime of polycarbonate surfaces, which for example are used as helmets or protective eye visors, friction and abrasive wear may result from scratching or sliding cycles. Previous research showed that it is essential to understand the intrinsic mechanical response of the polymer in order to further investigate its frictional and wear response. The Eindhoven Glassy Polymer (EGP) model is a 3D elasto-viscoplastic constitutive model, developed to describe the intrinsic mechanical response of polymer glasses. Temperature is a crucial player in the intrinsic response and also plays a pivotal role in the resulting frictional response as tested via a single-asperity scratch test. In the current study, a finite element model is used to investigate the effect of temperature on the frictional response of polycarbonate and detect the onset of crack formation and wear initiation. The results show that temperature has a strong effect on the intrinsic response of the polymer, i.e. drop in yield stress and altered strain-hardening and strain-softening response. However, it has a minute effect on its frictional response, the simulation model is able to capture this response quantitively. In addition, cracks are observed experimentally at elevated temperature. A critical positive hydrostatic stress value is selected as a criterion for crack formation. It has been shown that at elevated temperatures the value of the maximum positive hydrostatic stress increases due to the altered intrinsic response of the material on one hand, and the increased adhesion between the tip and the polymer on the other hand.

Keywords: Contact mechanics, Single-asperity sliding friction, Finite element modelling, Temperature

1. Introduction

Polymers display excellent tribological properties, they are often favoured above their metal counterparts in applications where friction and wear resistance are important. Polycarbonate (PC) is used in various applications such as face shields, protective glasses, facades or security windows in addition to many other automotive and consumer products. Here the polymer surface is subjected to a large number of scratching or sliding cycles which, over time, lead to abrasive wear, degradation and failure. This makes it necessary to study the frictional behaviour of the polymers. Many

*Corresponding author

Email address: L.C.A.v.Breemen@tue.nl (Lambèrt C.A. van Breemen[1])

studies aimed to investigate the tribology of polymers, however, due to complex contact conditions [1–4], and many experimental variables, the problem needs to be simplified. In order to do so, the single-asperity sliding test, known as scratch test, is used. It resembles the actual contact situation of the polymer product using a well-defined contact situation. The pioneering work of Bowden and Tabor [5] was the first to study the frictional response in which they presumed that the friction force can be additively decomposed into an adhesion and a deformation-related component.

Boyce et al.[6] developed a constitutive model describing the large inelastic deformation of glassy polymers in which the effects of strain rate, pressure, temperature, true strain softening, and strain hardening have been accounted for. As the Finite Element Method (FEM) started to emerge, benefiting from ongoing increase in computational power, new possibilities are now available to study non-linear contact problems. Larsson's group implemented a finite-strain constitutive material model in a FEM-framework to study the Vickers and Berkovic indentation of elasto-plastic materials [7, 8]. However, contact analysis for polymers is more complex due to their non-linear visco-elastic behaviour. Anand et al. [9] developed a continuum model for the elasto-viscoplastic deformation of an amorphous polymeric solid during micro-indentation, in which the FEM simulation reproduces the experimentally measured indentation on PMMA with reasonable accuracy. Van Breemen et al. [10] captured the rate and history dependence of polycarbonate and PMMA on both macroscopic and microscopic scale using flat-tip micro-indentation. The next step after indentation was to model the single-asperity scratching. Leroch et. al. [11] and Varga et. al. [12] used mesh-free numerical simulations such as Smoothed particle hydrodynamics (SPH) and Material Point Method (MPM) to simulate scratch-induced surface damage on an elasto-viscoplastic materials. These methods tackle the problem of severe deformations which is usually encountered in FEM simulations, however, they are computationally more expensive to use. Many studies aimed to analyse complex responses in sliding friction via experimental and numerical techniques [13–22]. Most provide a valuable description of the frictional response, but only on the qualitative level. The reason is that these studies imply that there is no dependence on strain rate of sliding velocity, and hence it does not correctly capture the visco-elastic pre-yield bahaviour of polymer glasses. The Eindhoven Glassy Polymer (EGP) model, which is a 3D elasto-viscoplastic model, was developed to describe the intrinsic mechanical response of polymers glasses [23–26]. Recently this model has been extended to capture the intrinsic response of polymer glasses with multiple relaxation times [27]. The work of Van Breemen et al. [28] and Krop et al. [29] used the EGP model to couple intrinsic material properties to the observed frictional response and investigate the effect of applied load and scratch velocity on the penetration and friction force on polycarbonate. The effect of temperature however, is still poorly understood when it comes to single-asperity scratching. It is expected that temperature has an influence on penetration and friction force during scratching due to the altered pre- and post-yield responses [30, 31].

The main objective of this study is using a hybrid experimental-numerical approach to investigate the effect of temperature during single-asperity scratching on the tribological properties of polycarbonate. Polycarbonate is selected as model material because of its well-defined mechanical properties and intrinsic response. The sample preparation and the scratch set-up and testing procedures are discussed in Section 2. We use the extended version of the EGP model [27], where the characterization of the intrinsic material properties is discussed in Section 3. Physical ageing

and mechanical rejuvenation have a profound influence on the scratch response which is taken care of in the model [32]. In the results section we compare numerical simulations with the experimental results to quantitatively describe the temperature effect on the frictional response of the polymer surface and predict the onset of crack formation.

2. Experimental

2.1. Materials and sample preparation

The material used in this study is Lexan 141R, a high molecular weight injection moulding grade polycarbonate (Sabic Innovative Plastics, Bergen op Zoom, The Netherlands). Samples of dimensions 20×20×1 mm^3 were cut from the centre of injection moulded plates, produced in a mould of 90 °C. The experimental protocol used to prepare these plates is given in more detail elsewhere [33]. After being stored at room temperature for over a year, the samples are dried for three days in a vacuum oven at 80 °C before being annealed for two weeks at a temperature of 120 °C. Subsequently the samples are air-cooled to room temperature under ambient conditions. The thermomechanical history as described above is needed to bring the material as close to equilibrium as possible, in order not to influence the thermodynamic state during scratch testing at elevated temperatures. The surface roughness of the samples is well below the threshold value of 1% of the in-situ surface penetration upon scratching, because of the polished interior of the mould. Optical profilometry as discussed in the next paragraph is used to validate that the surface roughness is considerably low and hence will not influence the lateral force measurement upon scratch testing.

2.2. Testing

Single-asperity sliding friction experiments are performed using a CSM Micro Indenter (CSM Instruments SA, Peseux, Switzerland) extended with an in-house developed temperature control stage. After setting the temperature to a specific value (23, 60 or 80 °C), the system is equilibrated for one hour before starting the actual measurements. Normal loads, ranging from 100-500 mN, are applied to the sample via a conical diamond indenter tip, with a cone angle of 90° and a top radius of 50 µm. A diamond indenter induces high contact-stress which resembles an extreme loading condition that a polycarbonate surface may be subjected to. The intention is to reach a contact stress above which cracks start to form and wear starts to initiate. After load application, a constant sliding velocity is applied, values of 1 µm/s, 10 µm/s, and 100 µm/s are used. The surface penetration and lateral friction force are measured as a function of scratch distance. Each combination of normal load and lateral sliding velocity is applied at least three times to check for reproducibility. All experimental results presented in the next section are averages of three scratches. Surface topologies before and after scratch experiments are measured using a Sensofar Plµ2300 optical profilometer (Sensofar Group, Barcelona, Spain). By using a setup of confocal lenses the sample is aligned horizontally, whereafter the system is moved over a distance of 20-40 µm in the out-of-plane direction. A Nikon Plan Fluor 50x/0.80 EPI lens is then used to construct three-dimensional patterns of the sample topology. Before the scratch tests are performed, a surface roughness in the order of 20 nm is measured. Post-mortem, the residual scratch profiles are measured by means of this technique.

3. Modelling

3.1. Constitutive model

The 3D elasto-viscoplastic constitutive model employed in this work consists of multiple Maxwell elements connected in parallel to a neo-Hookean spring. The model, see Van Breemen et al. [27] for more details, is based on an additive decomposition of the total stress $\boldsymbol{\sigma}$ into a driving stress $\boldsymbol{\sigma}_\mathrm{s}$ and a hardening stress $\boldsymbol{\sigma}_\mathrm{r}$:

$$\boldsymbol{\sigma} = \boldsymbol{\sigma}_\mathrm{s} + \boldsymbol{\sigma}_\mathrm{r}. \tag{1}$$

The hardening stress is modelled with a neo-Hookean spring and accounts for the stress contribution of the entangled molecular network:

$$\boldsymbol{\sigma}_\mathrm{r} = \frac{G_\mathrm{r}}{J}\tilde{\boldsymbol{B}}^\mathrm{d}, \tag{2}$$

herein, G_r denotes the hardening modulus, $\tilde{\boldsymbol{B}}^\mathrm{d}$ is the deviatoric part of the isochoric left Cauchy-Green strain tensor, and J is the volume change ratio. The driving stress is additively decomposed into a hydrostatic and deviatoric part:

$$\boldsymbol{\sigma}_\mathrm{s} = \boldsymbol{\sigma}_\mathrm{s}^\mathrm{h} + \boldsymbol{\sigma}_\mathrm{s}^\mathrm{d} = \kappa(J-1)\boldsymbol{I} + \sum_{i=1}^{n} G_i \tilde{\boldsymbol{B}}_{\mathrm{e},i}^\mathrm{d}, \tag{3}$$

where, κ is the bulk modulus, G is the shear modulus, $\tilde{\boldsymbol{B}}_\mathrm{e}^\mathrm{d}$ is the elastic deviatoric part of the isochoric left Cauchy-Green strain tensor, subscript i refers to a specific mode, and n denotes the number of modes. The deviatoric part $\boldsymbol{\sigma}_\mathrm{s}^\mathrm{d}$ is coupled to the plastic deformation rate tensor $\boldsymbol{D}_\mathrm{p}$ via a non-Newtonian flow rule:

$$\boldsymbol{D}_{\mathrm{p},i} = \frac{\boldsymbol{\sigma}_{\mathrm{s},i}^\mathrm{d}}{2\eta_i}, \tag{4}$$

where η_i are the viscosities of each Maxwell element which are described by the extended Eyring flow rule. This flow rule takes the pressure dependence and strain softening into account:

$$\eta_i = \eta_{0,\mathrm{ref},i}\frac{\bar{\tau}/\tau_0}{\sinh(\bar{\tau}/\tau_0)}\exp\left[\frac{\mu p}{\tau_0}\right]\exp[S_a R_x(\bar{\gamma}_\mathrm{p})], \tag{5}$$

where $\eta_{0,\mathrm{ref},i}$ are the reference viscosities of each Maxwell element, $\bar{\tau}$ is the total equivalent stress, τ_0 defines the characteristic shear stress, p is the hydrostatic pressure, the pressure dependency is governed by the parameter μ, the physical ageing is contained in the state parameter S_a. The function $R_x(\bar{\gamma}_\mathrm{p})$ describes the strain softening process using modified Carreau-Yasuda relation:

$$R_x(\bar{\gamma}_\mathrm{p}) = \left[\frac{1+(r_0.\exp(\bar{\gamma}_\mathrm{p}))^{r_1}}{1+r_0^{r_1}}\right]^{(r_2-1)/r_1}, \tag{6}$$

where $\bar{\gamma}_{\mathrm{p}}$ is the equivalent plastic strain, and r_0, r_1, and r_2 are the fitting parameters. When temperature is considered, τ_0 is determined using the following equation:

$$\tau_0 = \frac{kT}{V^*}, \tag{7}$$

where k is the Boltzmann's constant, V^* is the activation volume, and T represents the temperature. In addition, a temperature-dependent pre-exponential factor is added to the Eyring equation:

$$\eta_i = \eta_{0,\mathrm{ref},i} \frac{\bar{\tau}/\tau_0}{\sinh(\bar{\tau}/\tau_0)} \exp\left[\frac{\mu p}{\tau_0}\right] \exp[S_a R_x(\bar{\gamma}_{\mathrm{p}})] \exp\left[-\frac{\Delta U}{RT}\left(\frac{T - T_{\mathrm{ref}}}{T_{\mathrm{ref}}}\right)\right], \tag{8}$$

where ΔU is the activation energy, R is the universal gas constant, and T_{ref} is the room temperature.

3.2. Intrinsic response and model parameters

In order to obtain the model parameters of PC, the intrinsic response of the polymer is investigated. Single-element FEM compression simulations are performed and fitted to experiments. Figure 1a presents the strain-rate dependence of compressive stress-strain curves of PC. Upon an increase in strain rate the yield stress increases, and the post-yield response shifts accordingly. The polymer strain-rate dependency is relevant since the single-asperity scratch tests are performed at different scratch velocities, and the strain rate is not constant throughout the material. Consequently, the frictional response is dependent on the scratch velocity. Figure 1b shows the drop in yield stress which is observed at higher temperatures due to the softening of the polymer. As mentioned in the introduction, due to the drop in yield stress at elevated temperatures, more penetration and a higher friction force are expected in the scratch simulation. Moreover, the post-yield response changes as well; less strain softening and less strain hardening is observed at elevated temperatures. This post-yield response plays a determining role in strain localization [34, 35]. If the strain hardening is strong enough it stabilizes the deformation zones and resist the formation of localized plastic deformation zones caused by strain softening. Therefore, it is expected that such behaviour will contribute to localized strain accumulation during scratching and will increase the chance of crack formation especially at high normal loads. Figure 2 shows simulations and experimental yield stress values at different strain rates and temperatures. The experimental values are adopted from [36]. The slopes for different temperatures are similar, because PC is a thermorheologically simple material. This observation indicates that the dependence of the yield stress on strain rate and temperature can be separated and that there is no coupling effect between them. It is important to mention that PC has a secondary relaxation mechanism, however, this mechanism plays no role of importance at temperatures equal to, or above, room temperature provided that the deformation rates are moderate [37]. The thermodynamic state parameter S_a of the material is determined by using indentation simulations and fitting them to the experiments, analogous to [27]. Since our samples have been annealed at 120 °C for two weeks, the thermodynamic state parameter is relatively high; $S_a = 50$ as opposed to $S_a = 29$ for the compression samples. The high value of S_a results in a higher yield strength and larger

yield drop. The reflection of this in the single-asperity scratch tests is a decrease in the penetration due to this higher yield, and as a result, the friction force decreases. The obtained material parameters for PC are tabulated in Table 1, the relaxation spectra in Table 2, and the strain-hardening modulus and strain-softening fitting parameters are presented in Table 3 of Appendix A. The constitutive model is implemented in the FEM package MSC.Marc in order to simulate the single-asperity scratch test.

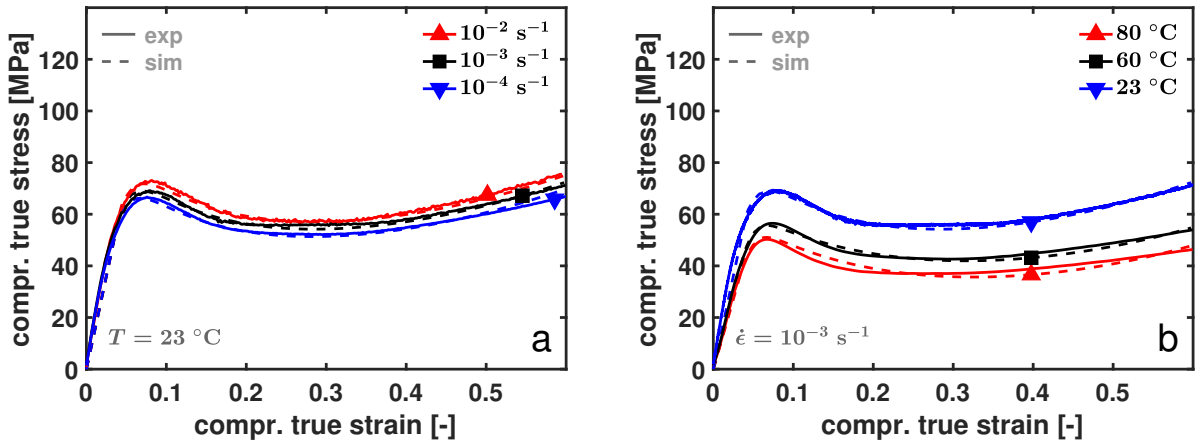

Figure 1: Uniaxial compression simulations results of PC (a) at different strain rates, (b) at different temperatures.

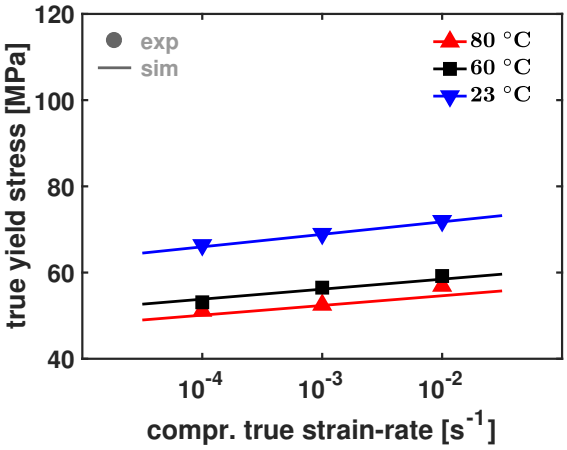

Figure 2: Yield stress of PC at various strain rates and temperatures. No coupling effect between rate dependency and temperature dependency.

3.3. Finite element mesh and friction modelling

The single-asperity scratch simulation is symmetric (Figure 3), therefore, only half of the polymer surface is meshed. The meshed volume is 0.2×0.2×0.8 mm^3. Although quadratic elements are often used to prevent shear

locking we use linear elements which are preferred in contact analysis [38]. The surface of the polymer has greatest interest, and is subjected to the highest stresses, so, mesh refinement is applied to this area. The symmetry plane is fixed in y-direction and the sides are restrained in x- and z-direction. A fixed uniform temperature distribution boundary condition is applied to the mesh; 23 °C, 60 °C, and 80 °C are applied to test the frictional response at these temperatures. The indenter tip radius is 50 µm, and is modelled as a rigid surface. The simulation is split in two parts, first indentation with constant normal load for 25 s, then sliding with constant velocity and normal load.

The Coulomb friction model is used, and to avoid numerical singularities, the step function is approximated with an arctangent model:

$$\boldsymbol{f}_{\mathrm{t}} = -\mu_{\mathrm{f}} f_{\mathrm{n}} \frac{2}{\pi} \arctan\left[\frac{\|\boldsymbol{v}_{\mathrm{r}}\|}{\delta}\right] \boldsymbol{t}, \tag{9}$$

where $\boldsymbol{f}_{\mathrm{t}}$ and f_{n} are the friction and normal forces respectively, μ_{f} the local friction coefficient, $\boldsymbol{v}_{\mathrm{r}}$ is the relative sliding velocity, and $\boldsymbol{t}$ is the tangential vector. The value of δ dictates the value of the relative velocity below which sticking occurs. The smaller the value of δ the better the estimation of the friction force, however, it becomes more difficult to reach convergence. Van Breemen et al. [28] showed that the friction force strongly depends on the friction coefficient. A high friction coefficient results in more indenter-polymer sticking, which leads to the formation of a bow wave in front of the sliding tip. This bow wave causes the tip to be pushed out of the surface and drastically changes the deformation zone. Van Breemen et al. [28] used a friction coefficient value of $\mu_{\mathrm{f}} = 0.20$ for PC which gives a best representation of the experimental data, while Krop et al. [29] used a value of $\mu_{\mathrm{f}} = 0.25$, the difference solely comes from the differences in surface roughness of the tips used. In our case, a local friction coefficient value of $\mu_{\mathrm{f}} = 0.25$ is found to give the best description of the experimental scratching of polycarbonate at room temperature, and is kept constant at different scratch velocities and normal loads. At elevated temperatures however, we test the possibility of increasing the friction coefficient due to the expected increased adhesion at these temperatures.

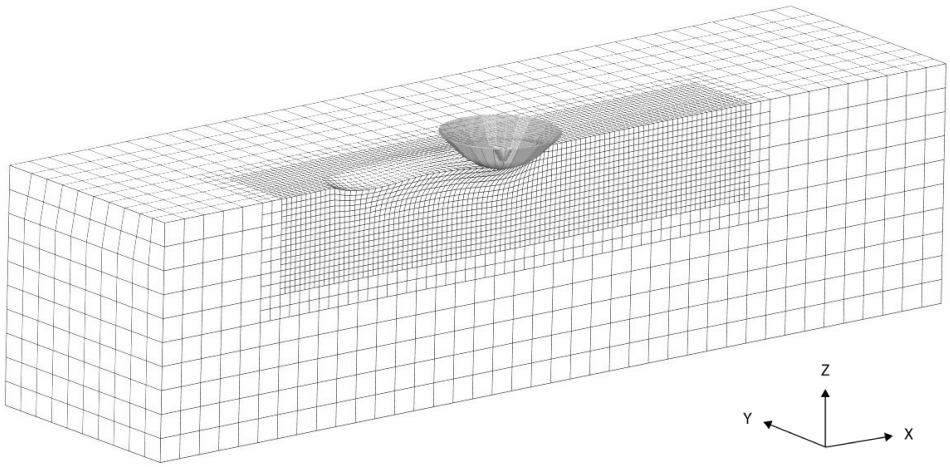

Figure 3: FEM mesh of single-asperity scratch simulation.

4. Results and Discussion

4.1. Scratch and frictional response

Scratch tests are performed at room temperature and two elevated temperatures; 60 °C and 80 °C, and at three different normal loads; 100 mN, 300 mN, and 500 mN, and three different scratch velocities; 1 µm/s, 10 µm/s, and 100 µm/s. The typical single-asperity scratch response is shown in Figure 4. Figure 4a presents the value of tip penetration into the polymer after indentation till it reaches the steady state. Figure 4b displays the corresponding frictional response. During simulation, the friction force takes longer time to reach steady state compared to experiments. The reason is the use of the approximated arctangent model to smoothen the stick-slip transition. In this model the parameter δ dictates the value below which sticking occurs, this value is around 10% of the relative velocity. In reality however, the stick-slip transition happens more abruptly leading to friction force build-up more rapidly. Simulations accurately capture the experimental response at room temperature, however, at elevated temperatures the penetration is overestimated, and the friction force is underestimated. This observation suggests that the local friction coefficient value of $\mu_f = 0.25$ is accurate at room temperature, however, at high temperatures it seems that there is more adhesion which leads to more friction between the tip and the polymer resulting in more material accumulation in front of the tip (bow wave). This pile-up of material in front of the tip increases the friction force and pushes the tip upwards. Figure 5 shows the experimental (a) and simulation data (b) of the indenter penetration into the surface of the polymer

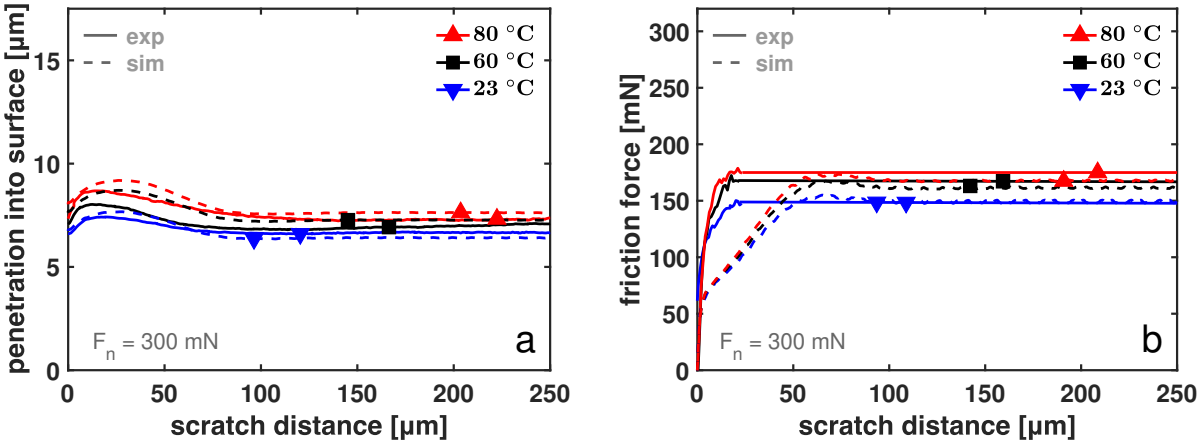

Figure 4: Single-asperity scratch results of PC at 100 µm/s scratch velocity ; (a) penetration into the surface versus sliding distance, (b) friction force versus sliding distance. Simulations accurately capture the experimental response at room temperature, however, at elevated temperatures the penetration is overestimated, and the friction force is underestimated.

at various normal loads and scratch velocities with the resulting frictional response illustrated in Figures 5c and 5d. Generally speaking, higher loads, lower scratch velocities, and higher temperatures introduce more mesh deformation and convergence becomes challenging. For this reason, when convergence cannot be reached, the fitting lines of simulations are extrapolated and the values are plotted using open markers. At higher applied loads we observe more

penetration and friction force. The same happens at lower scratch velocity due to the strain-rate dependency that results from the visco-elastic nature of the polymer. In other words, at low scratch velocity there is less material resistance to the indenter motion, so, it penetrates more into the surface, and more polymer gets in contact with the indenter resulting in an increased friction force. Higher temperatures lower the yield stress of the material and the post-yield response changes as well, i.e. less strain softening and less strain hardening, leading to more penetration and friction force. The observation of underestimation of friction force with overestimation of penetration depth at elevated temperatures is observed in almost all cases making the need for friction coefficient adjustment at elevated temperatures plausible.

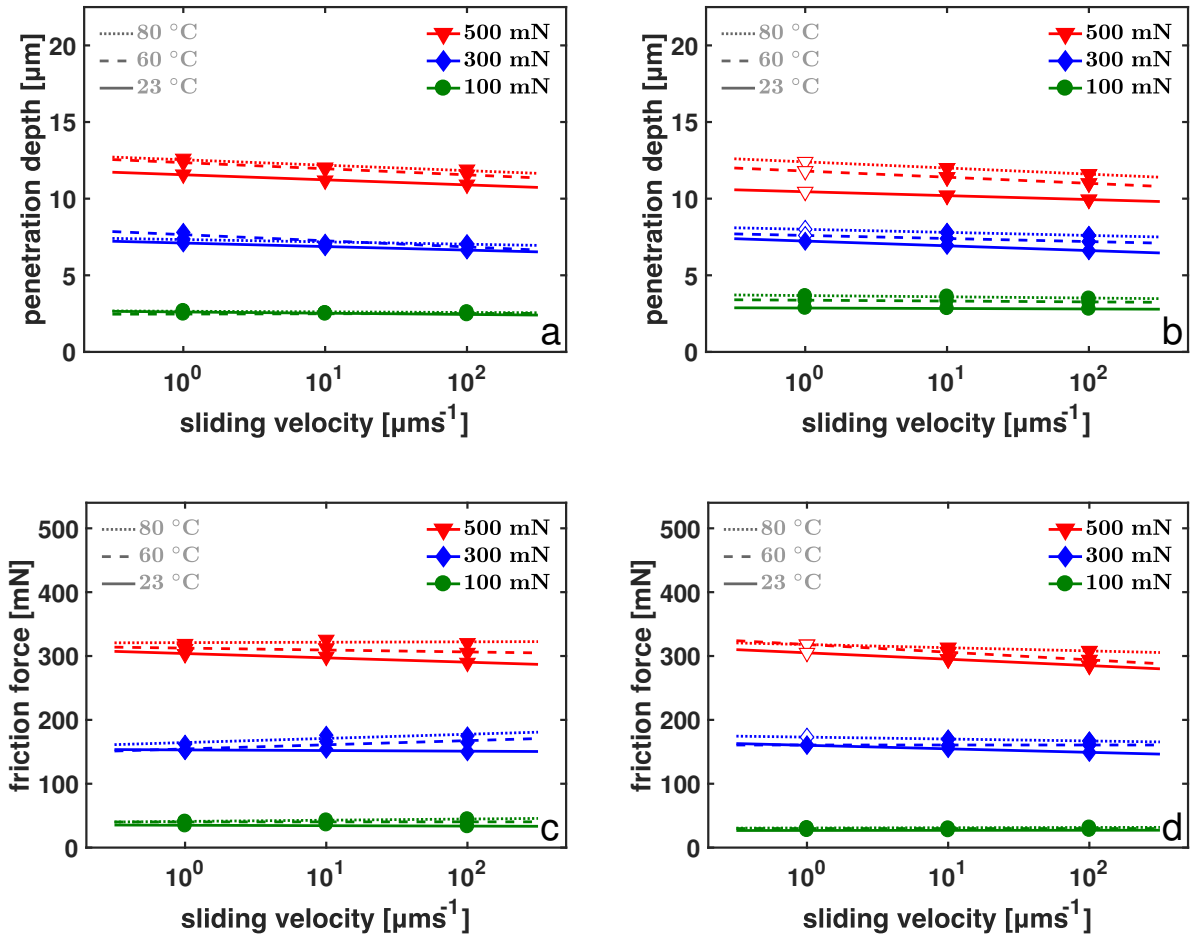

Figure 5: Penetration into the surface versus sliding distance of PC using a 50 µm tip at 100 mN, 300 mN, and 500 mN, and scratch velocities; 1 µm/s, 10 µm/s, and 100 µm/s; (a) experiments, (b) simulations. The resulting friction force; (c) experiments, (d) simulations. Lines are a guide to the eye. Open marker are extrapolated simulation values.

4.2. Friction coefficient

It has been reported that friction coefficient is temperature dependent for some materials [39]. A rational based on the fact that high temperatures lead to more adhesion between the polymer and the tip, resulting in more friction. From the previous results in Figures 4a and 4b it has been shown that our simulation underestimates the friction force at elevated temperatures. Instead of using a friction coefficient value of $\mu_f = 0.25$ at 60 °C and 80 °C degrees, vaules of $\mu_f = 0.27$ and $\mu_f = 0.28$ are used respectively. The scratch response at these values shows a better estimation of the penetration depth Figure 6a, this results from the bigger bow wave formed in front of the material due to increased adhesion, therefore, pushing the indenter up. As a result of the material pile-up, more material gets in contact with the tip increasing the friction force. The friction force values show better agreement with the experimental data, see Figure 6b. The entire stress field around the indenter changes as the friction coefficient increases at elevated temperatures.

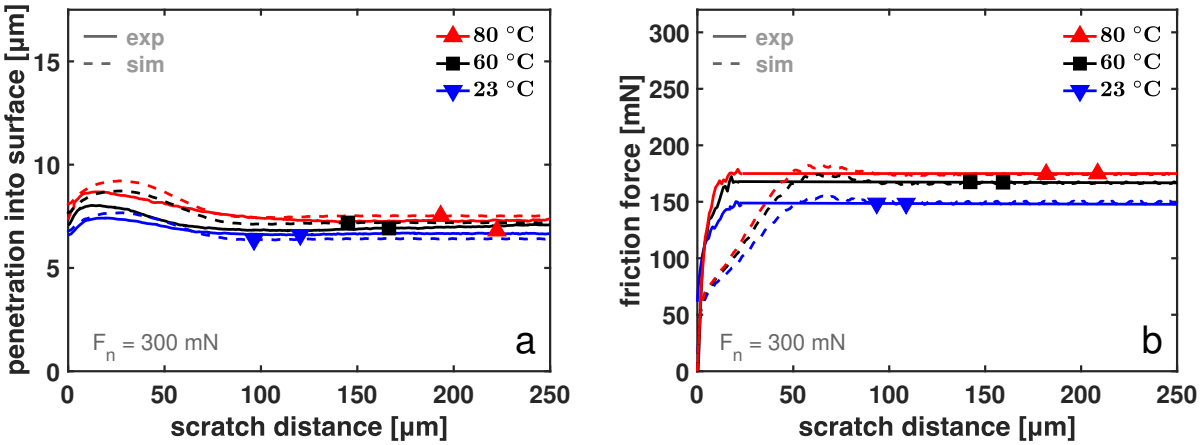

Figure 6: Simulation results of single-asperity scratch test of PC at 100 µm/s scratch velocity using a friction coefficient value of $\mu_f = 0.25$ at room temperature and $\mu_f = 0.27$ and $\mu_f = 0.28$ at 60 °C and 80 °C degrees respectively; (a) penetration into the surface versus sliding distance, (b) friction force versus sliding distance.

Figure 7a shows a 3D view of the mesh after single-asperity scratching at 300 mN, scratch velocity of 100 µm/s, and a temperature of 80 °C. A higher stress is observed using higher friction coefficient resulting from an increased adhesion and resistance of smooth tip movement, see Figure 7b. The increase of adhesion creates more sticking and accumulates the material infront of the tip which obstructs the horizontal movement of the tip and introduces an additional friction force. With less friction and resistance force, the tip will slip, i.e. move smoother. Now that we adjusted our friction coefficient at elevated temperatures, the new penetration response values at 300 mN normal load are shown in Figures 8a and 8b with the resulting frictional response illustrated in Figures 8c and 8d. The new results show better agreement of both the penetration depths and friction force at elevated temperatures. At elevated temperatures, two counteracting effects take place; material softens and friction coefficient, i.e. adhesion increases. The softening of the material leads to more surface penetration, whereas the increased adhesion leads to increased frictional shear stress along the contact surface which pushes the tip upwards. This is why temperature has little effect

on surface penetration. However, the significant increase in lateral force, despite the decrease in penetration, results from the formation of a bow wave in front of the sliding tip. This proves that the hypothesized friction coefficient dependency on temperature is valid.

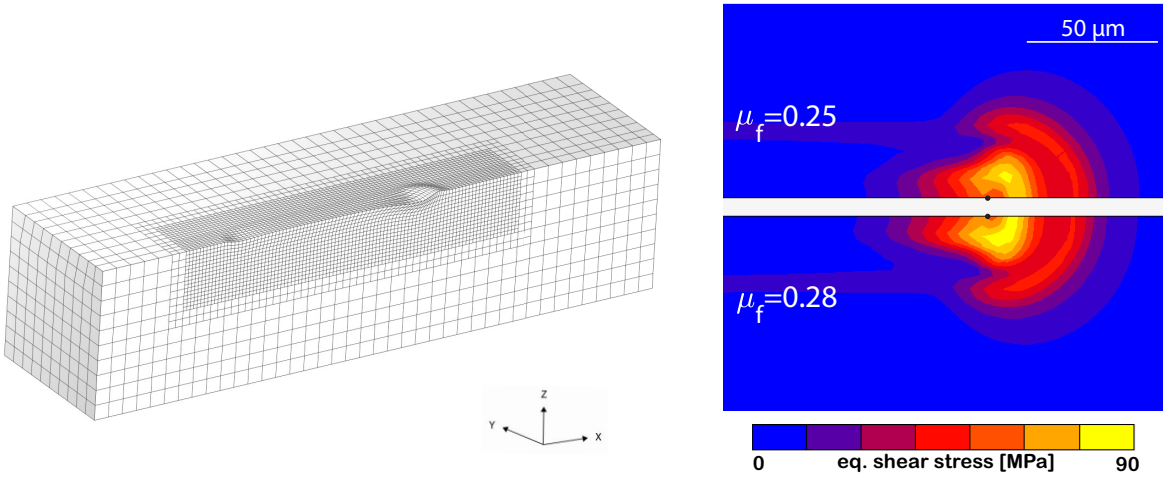

(a) (b)

Figure 7: (a) A 3D view of the mesh after single-asperity scratching of 300 mN normal load, scratch velocity 100 µm/s, and temperature 80 °C. (b) The equivalent shear stress field when looking at - Z-direction using friction coefficient value of μ_f = 0.25 (top) and μ_f = 0.28 (bottom). Black dot represents the tip centre. More stress is observed using higher friction coefficient resulting from more adhesion and resistance of smooth tip movement.

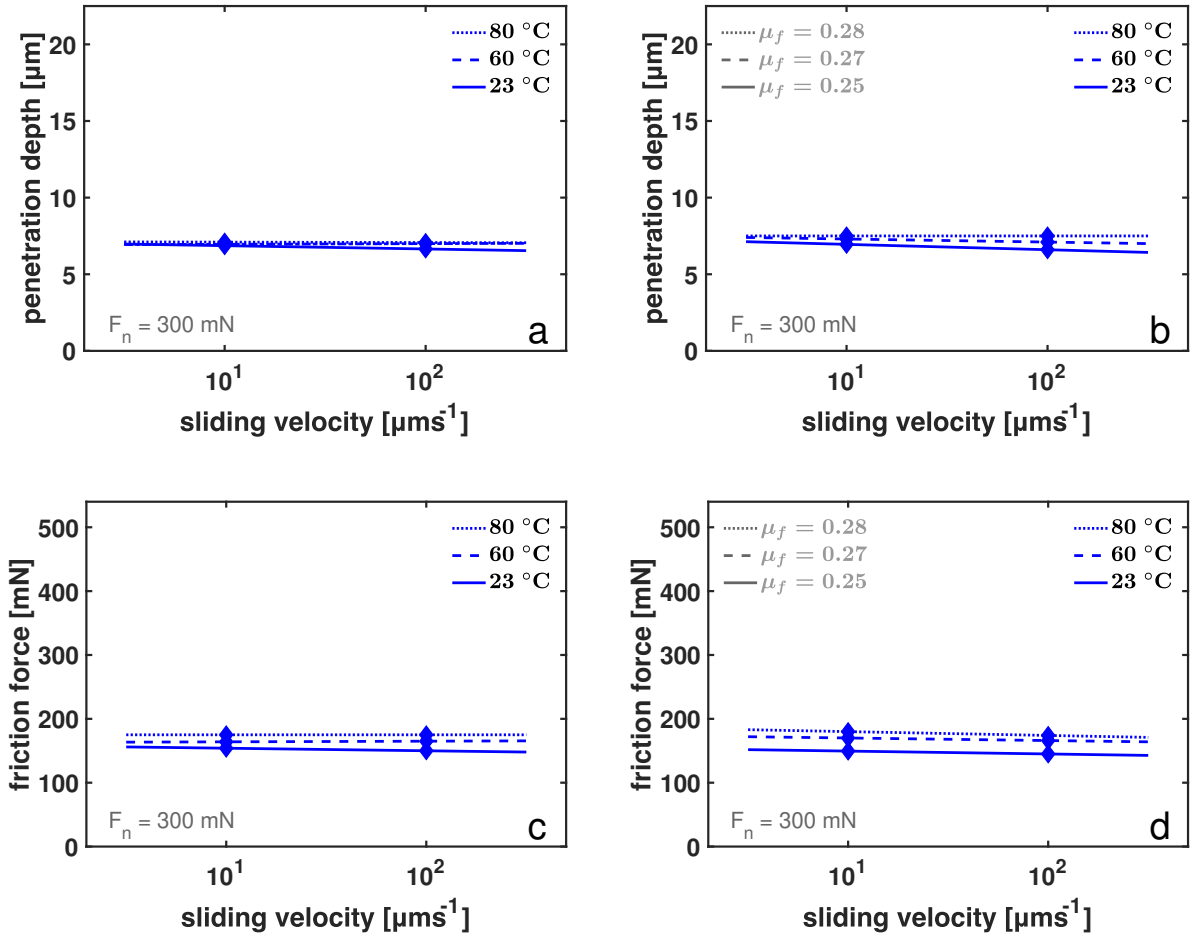

Figure 8: Penetration into the surface versus sliding distance of PC using a 50 µm tip at 300 mN, and scratch velocities; 10 µm/s, and 100 µm/s, using adjusted friction coefficient values at elevated temperatures; (a) experiments, (b) simulations. The corresponding friction force; (c) experiments, (d) simulations. Lines are a guide to the eye.

4.3. Crack formation

It has been reported that failure on polycarbonate surfaces initiates when a critical positive hydrostatic stress is reached [40–42]. These critical values can be reached earlier by increasing normal load, decreasing sliding velocities, or increasing temperatures. In this work we are interested in studying the effect of temperature on the friction and crack formation on polycarbonate surfaces. Figure 9 shows that cracks start to appear at 80 °C. Temperature rise leads to a change in the intrinsic response of the polymers as has been shown in Figure 1b. A drop in yield stress is observed at elevated temperature accompanied by a change in the balance between strain softening and strain hardening. The drop in yield stress leads to materials softening, which in principle allows the indenter to go deeper into the polymer surface, creating a larger contact area between the tip and polymer, leading to higher friction force values. However, as discussed before, this effect is counterbalanced by the increase in friction coefficient at elevated temperatures, leading to minor temperature dependence of the friction force and penetration depth. On the other hand, the change of balance between the strain softening and strain hardening, i.e. less strain softening and less strain hardening, results in localized plastic deformation. In single-asperity scratching this leads to localized strain accumulation during scratching, and enhancing the formation of cracks. However, the change in the intrinsic response is not the only determining factor for crack formation. In the previous subsection it is proven that the friction coefficient is temperature-dependent and might have a role in the formation of cracks. This rationale is based on the fact that an increase in friction coefficient results in more adhesion enhancing the formation of bow wave, i.e. material pile-up in front of the tip, and transition between stick and slip becomes less smooth which leads to change in the entire stress field as shown earlier. This change is expected to increase the positive hydrostatic stress as the material suddenly slips under the indenter. Since cracks start to appear at the load case of 300 mN and 10 µm/s at 80 °C, this load case is selected and compared with the same situation but at room temperature. As mentioned earlier, a critical positive hydrostatic stress will be used as

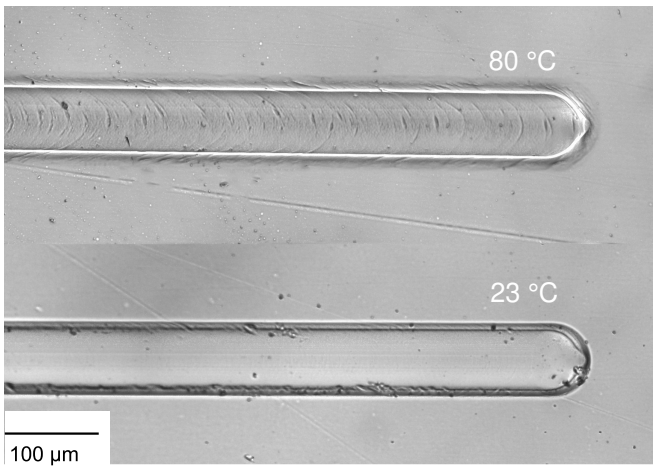

Figure 9: Scratch on PC surfaces at 300 mN and 10 µm/s at room temperature and 80 °C. Crack formation barely starts to appear at 80 °C.

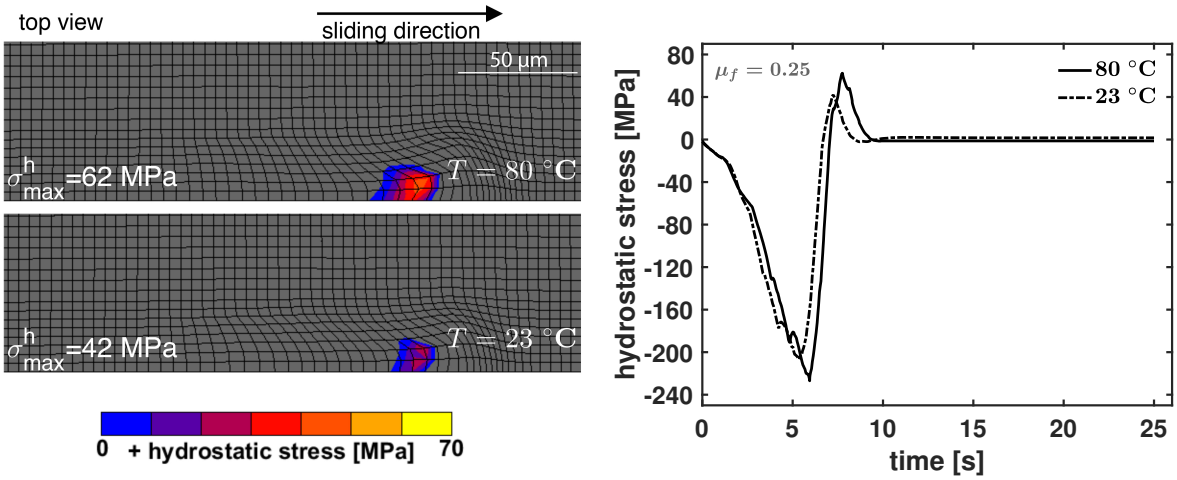

(a) (b)

Figure 10: (a) FEM simulation showing the values of positive hydrostatic stress along the surface when looking at - Z-direction at 80 °C and 23 °C at 300 mN and 10 µm/s, (b) evolution of hydrostatic stress along a selected element in the middle of the scratch surface for both cases. Friction coefficient μ_f=0.25 is used for both cases.

a criterion for crack formation. This critical value is approximately 80 MPa for Polycarbonate [40]. It is shown that at room temperature the value of the maximum positive hydrostatic stress σ^{h}_{max} = 42 MPa, while at 80 °C the value is σ^{h}_{max} = 62 MPa, with both cases at friction coefficient value of μ_f = 0.25, see Figure 10. The increase in the hydrostatic stress comes solely, in this case, from the altered intrinsic response of the material at high temperature, i.e. the drop

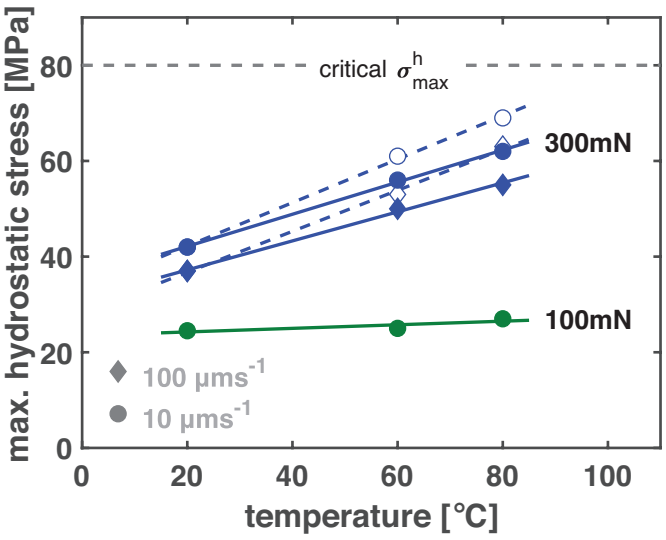

Figure 11: Maximum hydrostatic stress obtained by scratch simulations on PC at the indicated conditions. The solid lines represent the simulations performed with a friction coefficient of μ = 0.25. The dashed lines correspond to the simulations where the friction coefficient is temperature dependent. The open symbols belonging to the dashed lines indicate the simulation conditions at 60 °C with μ = 0.27 and at 80 °C with μ = 0.28. The experimentally obtained critical hydrostatic stress for PC is indicated at the top.

in yield stress in addition to strain-hardening and strain-softening imbalance, which leads to strain localization during scratching resulting in more penetration and a higher friction force. Figure 11 shows the temperature dependence of the maximum hydrostatic stress observed in the simulations. In case the deformation is mainly elastic, i.e. at an applied load of 100 mN, the maximum hydrostatic stress is independent of temperature and sliding velocity. When the normal load is increased, due to the difference in the post-yield deformation response, the maximum value strongly increases with increasing temperature. At lower sliding velocities, the hydrostatic stress values are larger compared to high scratch speeds, as a result of the viscoelastic nature of the material.

Next, we test the hypothesis of using a higher friction coefficient value at 80 °C with a value of $\mu_f = 0.28$. The resulting maximum hydrostatic stress value reaches $\sigma^h_{max} = 69$ MPa, see Figure 12. This increase represents about 25% of the total increase in the hydrostatic stress and pushes the total positive hydrostatic stress to its critical value. This percentage comes only from the altered interaction between the polymer-tip surface, i.e. more sticking and adhesion and a less smooth stick-slip transition. This increase is depicted in Figure 11 with dashed-lines. At 80 °C, this value becomes close to the critical hydrostatic stress. Experimentally, at these test conditions failure may be initiated because of inhomogeneities in the material, leading to stress concentrations. It should be noted that hydrostatic stress is a local variable and is dependent on mesh refinement. Although no full convergence is reached with the current level of mesh refinement, the change in maximum hydrostatic stress is small. Further increasing the level of refinement does not add much to the critical values reached, while it substantially increases the computational time. A further study of abrasive wear has been performed via investigating the abrasive wear factor f_{ab} first introduced by Zum Gahr [43] and used by Varga et. al. [44]. The factor is proven to give a value of $f_{ab} = 0$ at all loads, speeds and temperatures both experimentally and numerically. This implies that our scratch tests only involve ductile ploughing and no cutting, and that the cracks appearing at elevated temperatures do not involve any material loss.

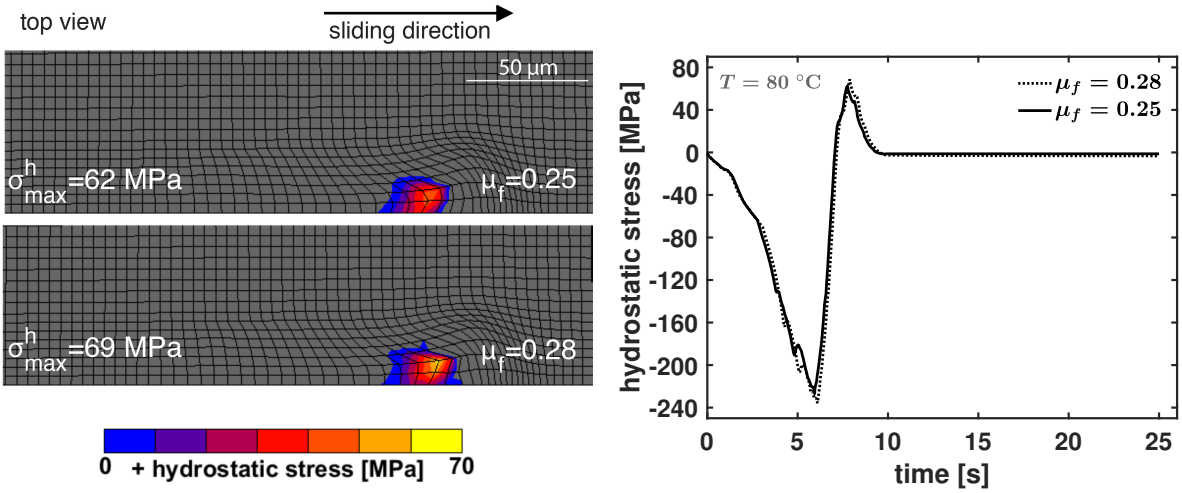

(a) (b)

Figure 12: (a) FEM simulation showing the values of positive hydrostatic stress along the surface when looking at - Z-direction at 80 °C using friction coefficient μ_f=0.25 and μ_f=0.28, (b) evolution of hydrostatic stress along a selected element in the middle of the scratch surface for both cases.

5. Conclusions

The hybrid experimental-numerical approach is successfully used to quantify the friction and abrasive-wear response of polycarbonate at room and elevated temperatures. The model has been implemented in a FEM-framework to test the intrinsic response of polycarbonate at various strain rates and temperatures. Successfully, FEM simulations of the single-asperity scratch test were performed and compared to experimental results. From the results we conclude that:

1. More tip penetration is observed at elevated temperatures due to the drop in intrinsic yield stress. This leads to an increased indenter-polymer contact area resulting in higher friction force.

2. The strain-rate dependency of the polymer leads to more resistance of the material to scratch at higher scratch velocities resulting in less penetration and frictional response.

3. Higher temperatures lower the yield stress of the material and the post-yield response changes as well, i.e. less strain softening and less strain hardening. This behaviour leads to the formation of localized plastic deformation zones and localized strain accumulation during scratching, which enhances the formation of cracks.

4. At high temperatures there is more adhesion which leads to more friction between the tip and the polymer resulting in more material accumulation in front of the tip. This pile-up of the material increases the friction force and pushes the tip upwards. Adjusting the friction coefficient at elevated temperature enables the model to accurately predict the resulting friction force.

5. A critical positive hydrostatic stress value is selected as a criterion for crack initiation . It has been shown that at elevated temperatures the value of the maximum positive hydrostatic stress increases solely from the altered intrinsic response of the material at these temperatures, given that the friction coefficient value is the same.

6. The hypothesized increase in the friction coefficient is tested to examine its effect on hydrostatic stress. The increased sticking and adhesion and less smooth stick-slip transition leads to higher positive hydrostatic stress values, which accounts for about 25% of the total increase observed. This means that the crack formation observed at elevated temperatures comes from the change in the intrinsic response on one hand, and the change in the polymer-tip interaction on the other hand.

Acknowledgements

This research forms part of the research programme of Dutch Polymer Institute (DPI), project 783t. The authors wish to thank DPI for their financial support.

Appendix A Material parameters

Table 1: Material parameters of PC.

κ [MPa]	S_a [-]	μ [-]	V^* [nm^3]	ΔU [kJ/mole]
3750	50	0.08	5.8	291

Table 2: Reference spectrum of PC, adopted from Van Breemen et al. [27].

Mode	$\eta_{0,\mathrm{ref},i}$ [MPa.s]	G_i [MPa]
1	2.10×10^{11}	3.52×10^{2}
2	3.48×10^{9}	5.55×10^{1}
3	2.95×10^{8}	4.48×10^{1}
4	2.84×10^{7}	4.12×10^{1}
5	2.54×10^{6}	3.50×10^{1}
6	2.44×10^{5}	3.20×10^{1}
7	2.20×10^{4}	2.75×10^{1}
8	2.04×10^{3}	2.43×10^{1}
9	1.83×10^{2}	2.07×10^{1}
10	1.68×10^{1}	1.81×10^{1}

Table 3: Strain-hardening modulus and strain-softening fitting parameters of PC as function of temperature.

	23 °C	60 °C	80 °C
G_r [MPa]	27	24	23
r_0 [-]	0.95	1	1
r_1 [-]	50	50	50
r_2 [-]	-3	-1.85	-1.6

References

References

[1] B. J. Briscoe, P. D. Evans, S. K. Biswas, S. K. Sinha, The hardnesses of poly(methylmethacrylate), Tribology International 29 (2) (1996) 93–104 (1996).

[2] B. J. Briscoe, E. Pelillo, S. K. Sinha, Scratch hardness and deformation maps for polycarbonate and polyethylene, Polymer Engineering and Science 36 (24) (1996) 2996–3005 (1996).

[3] B. J. Briscoe, Isolated contact stress deformations of polymers: The basis for interpreting polymer tribology, Tribology International 31 (1-3) (1998) 121–126 (1998).

[4] B. J. Briscoe, S. K. Sinha, Wear of polymers, Proceedings of the Institution of Mechanical Engineers, Part J: Journal of Engineering Tribology 216 (6) (2002) 401–413 (2002).

[5] F. P. Bowden, D. Tabor, Friction, lubrication and wear: A survey of work during the last decade, British Journal of Applied Physics 17 (12) (1966) 1521–1544 (1966).

[6] M. C. Boyce, D. M. Parks, A. S. Argon, Large inelastic deformation of glassy polymers. part i: rate dependent constitutive model, Mechanics of Materials 7 (1) (1988) 15–33 (1988).

[7] A. E. Giannakopoulos, P.-L. Larsson, R. Vestergaard, Analysis of vickers indentation, International Journal of Solids and Structures 31 (19) (1994) 2679–2708 (1994).

[8] P.-L. Larsson, A. E. Giannakopoulos, E. Söderlund, D. J. Rowcliffe, R. Vestergaard, Analysis of berkovich indentation, International Journal of Solids and Structures 33 (2) (1996) 221–248 (1996).

[9] L. Anand, N. M. Ames, On modeling the micro-indentation response of an amorphous polymer, International Journal of Plasticity 22 (6) (2006) 1123–1170 (2006).

[10] L. C. A. van Breemen, T. A. P. Engels, C. G. N. Pelletier, L. E. Govaert, J. M. J. den Toonder, Numerical simulation of flat-tip micro-indentation of glassy polymers: Influence of loading speed and thermodynamic state, Philosophical Magazine 89 (8) (2009) 677–696 (2009).

[11] S. Leroch, M. Varga, S. J. Eder, A. Vernes, M. R. Ripoll, G. Ganzenmüller, Smooth particle hydrodynamics simulation of damage induced by a spherical indenter scratching a viscoplastic material, International Journal of Solids and Structures 81 (2016) 188–202 (2016).

[12] M. Varga, S. Leroch, S. J. Eder, H. Rojacz, M. R. Ripoll, Influence of velocity on high-temperature fundamental abrasive contact: A numerical and experimental approach, Wear 426 (2019) 370–377 (2019).

[13] J. H. Lee, G. H. Xu, H. Liang, Experimental and numerical analysis of friction and wear behavior of polycarbonate, Wear 250-251 (2) (2001) 1541–1556 (2001).

[14] C. Gauthier, S. Lafaye, R. Schirrer, Elastic recovery of a scratch in a polymeric surface: Experiments and analysis, Tribology International 34 (7) (2001) 469–479 (2001).

[15] J. Bucaille, C. Gauthier, E. Felder, R. Schirrer, The influence of strain hardening of polymers on the piling-up phenomenon in scratch tests: Experiments and numerical modelling, Wear 260 (7-8) (2006) 803–814 (2006).

[16] H. Jiang, G. T. Lim, J. N. Reddy, J. D. Whitcomb, H.-J. Sue, Finite element method parametric study on scratch behavior of polymers, Journal of Polymer Science, Part B: Polymer Physics 45 (12) (2007) 1435–1447 (2007).

[17] N. Aleksy, G. Kermouche, A. Vautrin, J. M. Bergheau, Numerical study of scratch velocity effect on recovery of viscoelastic-viscoplastic solids, International Journal of Mechanical Sciences 52 (3) (2010) 455–463 (2010).

[18] H. Pelletier, C. Gauthier, R. Schirrer, Influence of the friction coefficient on the contact geometry during scratch onto amorphous polymers, Wear 268 (9-10) (2010) 1157–1169 (2010).

[19] Z. Wang, P. Gu, H. Zhang, Z. Zhang, X. Wu, Finite element modeling of the indentation and scratch response of epoxy/silica nanocomposites, Mechanics of Advanced Materials and Structures 21 (10) (2014) 802–809 (2014).

[20] M. M. Hossain, R. Minkwitz, P. Charoensirisomboon, H.-J. Sue, Quantitative modeling of scratch-induced deformation in amorphous polymers, Polymer 55 (23) (2014) 6152–6166 (2014).

[21] B. Feng, Z. Chen, Tribology behavior during indentation and scratch of thin films on substrates: Effects of plastic friction, AIP Advances 5 (5) (2015).

[22] J. Zhang, H. Jiang, C. Jiang, G. Kang, Q. Kan, Y. Li, Experimental and numerical investigations of evaluation criteria and material parameters' coupling effect on polypropylene scratch, Polymer Engineering & Science 58 (1) (2018) 118–122 (2018).

[23] R. N. Haward, G. Thacray, Use of a mathematical model to describe isothermal stress-strain curves in glassy thermoplastics, Proceedings of the Royal Society of London Series 302 (1471) (1968) 453–472 (1968).

[24] T. A. Tervoort, E. T. J. Klompen, L. E. Govaert, A multi-mode approach to finite, three-dimensional, nonlinear viscoelastic behavior of polymer glasses, Journal of Rheology 40 (5) (1996) 779–797 (1996).

[25] T. A. Tervoort, R. J. M. Smit, W. A. M. Brekelmans, L. E. Govaert, A constitutive equation for the elasto-viscoplastic deformation of glassy polymers, Mechanics Time-Dependent Materials 1 (3) (1997) 269–291 (1997).

[26] L. E. Govaert, P. H. M. Timmermans, W. A. M. Brekelmans, The influence of intrinsic strain softening on strain localization in polycarbonate: Modeling and experimental validation, Journal of Engineering Materials and Technology, Transactions of the ASME 122 (2) (2000) 177–185 (2000).

[27] L. C. A. van Breemen, E. T. J. Klompen, L. E. Govaert, H. E. H. Meijer, Extending the EGP constitutive model for polymer glasses to multiple relaxation times, Journal of the Mechanics and Physics of Solids 59 (10) (2011) 2191–2207 (2011).

[28] L. C. A. van Breemen, L. E. Govaert, H. E. H. Meijer, Scratching polycarbonate: A quantitative model, Wear 274-275 (2012) 238–247 (2012).

[29] S. Krop, H. E. H. Meijer, L. C. A. van Breemen, Finite element modeling and experimental validation of single-asperity sliding friction of diamond against reinforced and non-filled polycarbonate, Wear 356-357 (2016) 77–85 (2016).

[30] T. A. P. Engels, L. E. Govaert, H. E. H. Meijer, The influence of molecular orientation on the yield and post-yield response of injection-molded polycarbonate, Macromolecular Materials and Engineering 294 (12) (2009) 821–828 (2009).

[31] L. C. A. van Breemen, T. A. P. Engels, E. T. J. Klompen, D. J. A. Senden, L. E. Govaert, Rate-and temperature-dependent strain softening in solid polymers, Journal of Polymer Science Part B: Polymer Physics 50 (24) (2012) 1757–1771 (2012).

[32] E. T. J. Klompen, T. A. P. Engels, L. E. Govaert, H. E. H. Meijer, Modeling of the postyield response of glassy polymers: Influence of thermomechanical history, Macromolecules 38 (16) (2005) 6997–7008 (2005).

[33] T. A. P. Engels, B. A. G. Schrauwen, L. E. Govaert, H. E. H. Meijer, Improvement of the long-term performance of impact-modified polycarbonate by selected heat treatments, Macromolecular Materials and Engineering 294 (2) (2009) 114–121 (2009).

[34] H. G. H. van Melick, L. E. Govaert, H. E. H. Meijer, Localisation phenomena in glassy polymers: Influence of thermal and mechanical history, Polymer 44 (12) (2003) 3579–3591 (2003).

[35] H. E. H. Meijer, L. E. Govaert, Mechanical performance of polymer systems: The relation between structure and properties, Progress in Polymer Science 30 (8-9) (2005) 915–938 (2005).

[36] D. J. A. Senden, S. Krop, J. A. W. van Dommelen, L. E. Govaert, Rate- and temperature-dependent strain hardening of polycarbonate, Journal of Polymer Science, Part B: Polymer Physics 50 (24) (2012) 1680–1693 (2012).

[37] C. Bauwens-Crowet, J.-C. Bauwens, G. Homès, The temperature dependence of yield of polycarbonate in uniaxial compression and tensile tests, Journal of Materials Science 7 (2) (1972) 176–183 (1972).

[38] MSC Software MSC Marc: Element Library Volume B, MSC.Software GmbH (2014).

[39] G. Wróbel, M. Szymiczek, Influence of temperature on friction coefficient of low density polyethylene, Journal of Achievements in Materials and Manufacturing Engineering 28 (1) (2008) 31–34 (2008).

[40] T. A. P. Engels, L. C. A. van Breemen, L. E. Govaert, H. E. H. Meijer, Criteria to predict the embrittlement of polycarbonate, Polymer 52 (8) (2011) 1811–1819 (2011).

[41] R. P. Nimmer, J. T. Woods, Investigation of brittle failure in ductile, notch-sensitive thermoplastics, American Society of Mechanical Engineers, Materials Division 29 (1991) 129–148 (1991).

[42] S. F. S. P. Looijmans, V. G. de Bie, P. D. Anderson, L. C. A. van Breemen, Hydrostatic stress as indicator for wear initiation in polymer tribology, Wear 426-427 (2019) 1026–1032 (2019).

[43] K.-H. Zum Gahr, Microstructure and wear of materials, Vol. 10, Elsevier, 1987 (1987).

[44] M. Varga, S. Leroch, S. J. Eder, M. R. Ripoll, Meshless microscale simulation of wear mechanisms in scratch testing, Wear 376 (2017) 1122–1129 (2017).